

Electron Microscopy Study of $K_xBa_{1-x}NbO_3$

C. Chaillout,^{*,1} E. Gautier,* E. M. Kopnin,[†] T. Fournier,* E. V. Antipov,[†] and M. Marezio^{*,‡}

^{*}Laboratoire de Cristallographie, CNRS-UJF, BP 166, 38042 Grenoble Cedex 09, France; [†]Department of Chemistry, Moscow State University, 119899 Moscow, Russia; and [‡]AT&T Bell Laboratories, Murray Hill, New Jersey 07974

Received August 7, 1995; in revised form February 5, 1996; accepted February 8, 1996

$Ba_{1-x}K_xNbO_3$ ($x = 0$ and $x = 0.4$) samples have been studied by electron microscopy. Diffraction patterns as well as high resolution images of the $x = 0$ sample showed the presence of small misoriented domains. From energy dispersive spectroscopy (EDS) analysis the (Ba + K)/Nb ratio was found to be equal to 1. Neither superstructure reflections nor distortion from the cubic symmetry was detected. © 1996 Academic Press, Inc.

INTRODUCTION

Recently, we synthesized $K_xBa_{1-x}NbO_3$ compounds with $x = 0$ and $0.2 \leq x \leq 0.5$ (1). They were chosen because of the mixed valence state of niobium. This could lead to interesting transport properties including superconductivity, although this property has never been observed in Nb mixed oxides with Nb valence higher than 4+ (2–7).

The K-doped samples were prepared at high temperature and under high pressure in a belt-type apparatus, whereas $BaNbO_3$ was obtained in sealed silica tubes. However, some $BaNbO_3$ samples were submitted to subsequent high pressure high temperature treatments.

The different samples were studied by X-ray powder diffraction, a.c. susceptibility, and resistivity, as well as electron microscopy. Resistivity measurements showed that the K-doped samples had a semiconducting-like behavior, whereas $BaNbO_3$ exhibited a metallic-like conductivity down to 4.2 K. From X-ray powder diffraction, all phases were found to have a perovskite-like structure with no distortion of the cubic symmetry. However, the width of the main hkl reflections was larger than expected, especially for the undoped compound, and was found to increase monotonically with the diffraction angle. The detailed results concerning the physical properties and the X-ray diffraction analysis have already been reported in reference (1).

This paper reports the electron microscopy studies (electron diffraction, high resolution images (HREM), and electron dispersive spectroscopy analysis (EDS)) of $BaNbO_3$

before and after pressure treatment and of $K_{0.5}Ba_{0.5}NbO_3$. The aim of the present contribution was first of all to detect the possible presence of a small distortion from the cubic symmetry. In the case of $K_{0.5}Ba_{0.5}NbO_3$ this distortion could be related to a localization of Nb^{IV} and Nb^V cations on independent crystallographic sites. The second point was to determine the cation stoichiometry by EDS analysis to see if the K distribution was homogeneous and to check the (Ba + K)/Nb ratio. The last point was to study the presence of defects in the samples.

EXPERIMENTAL

Samples corresponding to the nominal stoichiometries $BaNbO_3$ (as-synthesized, sample 1, and high pressure treated, sample 2) and $K_{0.5}Ba_{0.5}NbO_3$ (sample 3) were prepared as described in (1). Electron microscopy study was performed on a Philips CM 300 microscope operating at 300 kV, with a Scherzer resolution limit of 1.9 Å, and equipped with a KeveX EDS analysis system (sigma). The samples were prepared by grinding the powders in alcohol and the crystallites were recovered from the suspension on a holey carbon film. HREM images were calculated for different thicknesses and different defocus values by using the EMS program (8).

RESULTS

1. EDS Analysis

For all samples, the cation stoichiometry was determined by analyzing several crystallites including those used for electron diffraction patterns and HREM images. The k factors used in the EDS analysis were determined from analyses of $Ba_5Nb_4O_{15}$ and $KNbO_3$.

In samples 1 and 2, the Ba/Nb ratio was found to be equal to 1 (within the standard deviations) for all studied crystallites. A Ba deficiency was reported previously for $BaNbO_3$ (9).

In sample 3, the (Ba + K)/Nb ratio was also equal to 1 and the Ba/K ratio varied between 0.8 and 1 which occurred for most of the crystallites. These limits correspond to $K_{0.56}Ba_{0.44}NbO_3$ and $K_{0.5}Ba_{0.5}NbO_3$, respectively.

¹ To whom correspondence should be addressed.

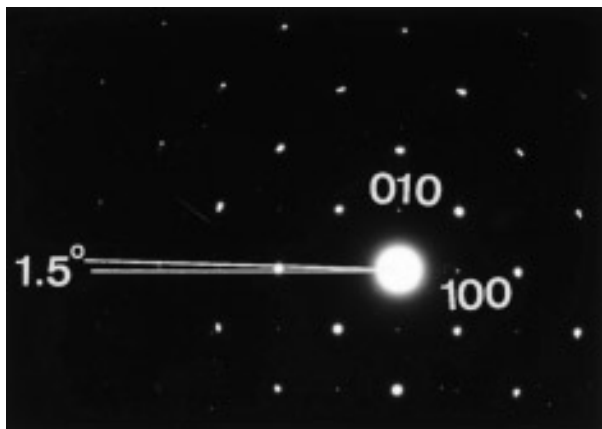


FIG. 1. Electron diffraction pattern taken along the $\langle 001 \rangle$ zone axis of an as-synthesized $BaNbO_3$ crystallite. The diffraction spots appear split.

2. Electron Diffraction

Diffraction patterns were taken along $\langle 001 \rangle$, $\langle 110 \rangle$, and $\langle 111 \rangle$ zone axes, for $BaNbO_3$, before and after pressure treatment (samples 1 and 2), and sample 3. All spots can be indexed by using the cubic cell parameter $a \approx 4.090 \text{ \AA}$ obtained from powder X-ray diffraction data. For samples 1 and 2 the diffraction spots appeared elongated and in some cases split. As an example, the pattern along the $\langle 001 \rangle$ zone axis of sample 2 is given in Fig. 1. The angle measured on the diffraction pattern between two neighboring spots along a^* is about 1.5° . The sample angle for sample 1 is smaller, about 0.5° . Most of the crystallites did not show any splitting for the K-doped sample.

In the case of the K-doped sample, we looked for superstructure reflections in diffraction patterns taken along the $\langle 100 \rangle$ and $\langle 110 \rangle$ zone axes, but no additional reflections were observed that could be related to a Ba–K or a Nb^{IV} – Nb^V ordering. Regarding the large difference between Ba (56) and K (19) atomic numbers, a Ba–K ordering would have been visible by X-ray diffraction if present. However, electron diffraction is known to be sensitive to ordering phenomena occurring on smaller scales than those detected by X ray.

3. High Resolution Images

a. $BaNbO_3$. Figure 2 shows an image taken along the $\langle 111 \rangle$ zone axis of a crystallite of sample 2. In this orientation, the Ba and Nb atoms which occupy the (000) and $(1/2 \ 1/2 \ 1/2)$ sites in the $Pm\bar{3}m$ space group, respectively, are projected on top of each other. They are imaged as white dots (image taken at Scherzer defocus). It can be seen that the dots are not well aligned over long distances but they form broken lines. The domain size where the orientation is constant is about 15 \AA . Images of the same sample but taken along the $\langle 001 \rangle$ zone axis show the same

domain pattern. An example is given in Fig. 3, taken at a defocus of $\approx -700 \text{ \AA}$. From image calculations, this experimental image would correspond to an area of about 20–40 \AA thick, and Ba and Nb cannot be distinguished. The misorientation between adjacent domains, measured along the $[110]$ direction, is about 3° , which is in agreement with the splitting observed on diffraction patterns for the same sample. In the regions between the grains the contrast is more diffuse. Inside a given domain, no deformation from perfect cubic symmetry was detected since the $\langle 110 \rangle$ directions were exactly at 60° from each other.

HREM taken along $\langle 001 \rangle$ and $\langle 111 \rangle$ zone axes for sample 1 (as-synthesized $BaNbO_3$) indicate that misoriented grains are also present before the pressure treatment but the misorientation is smaller and the size of the domains is somewhat larger ($\approx 40 \text{ \AA}$) than in sample 2. These observations allow us to understand the broadness of the reflections observed by X-ray diffraction (1). The higher the misorientation between the grains is, and the smaller the domains are, the higher the strain in the sample is, and

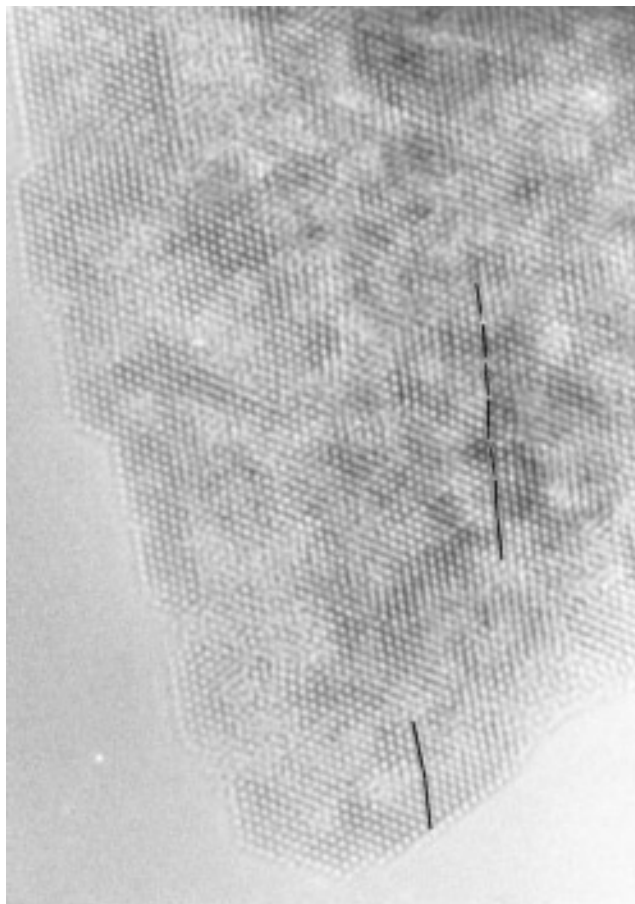


FIG. 2. HREM image of $BaNbO_3$ (sample 2) taken along the $\langle 111 \rangle$ zone axis close to Scherzer defocus. The misorientation between domains is outlined by the broken line on the image.

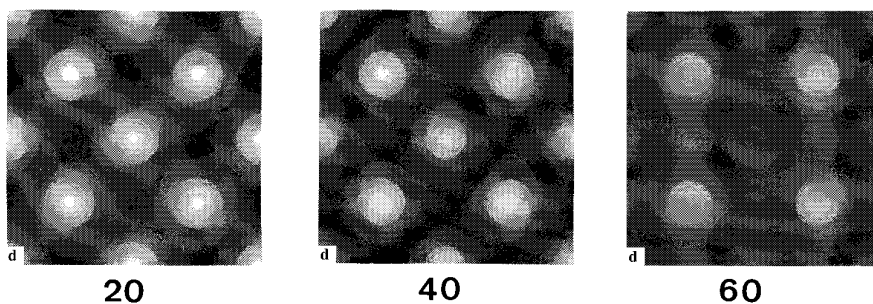
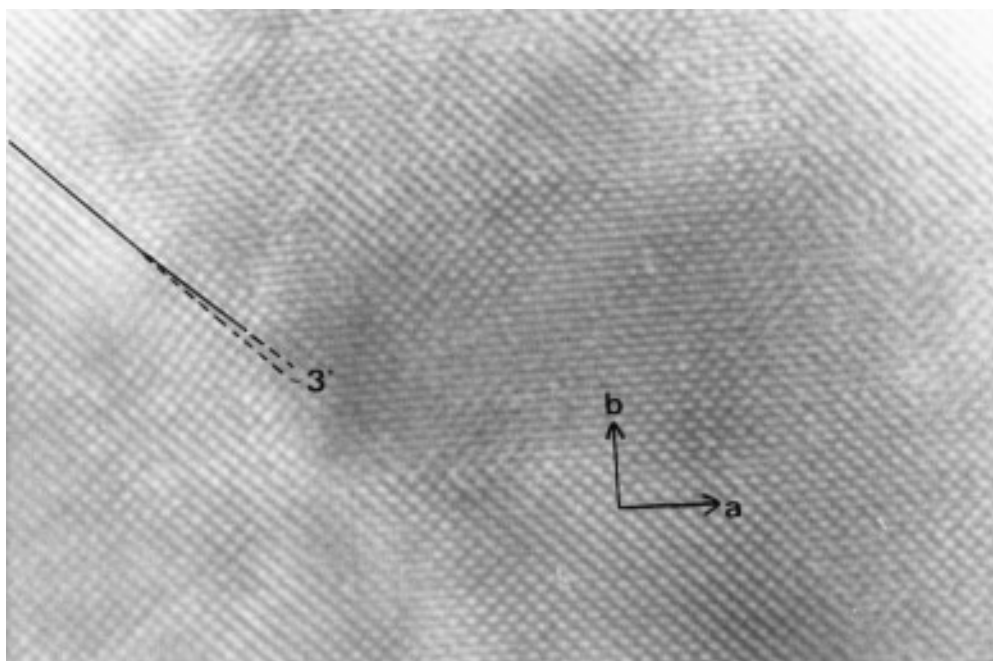


FIG. 3. HREM image of BaNbO_3 (sample 2) taken along the $\langle 001 \rangle$ zone axis (defocus $\approx -700 \text{ \AA}$).

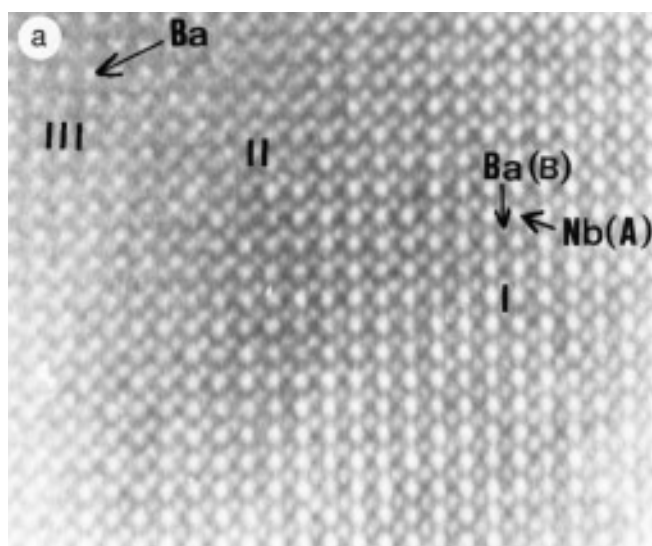


FIG. 4. (a) HREM image of $\text{Ba}_{0.5}\text{K}_{0.5}\text{NbO}_3$ (sample 3) taken along the $\langle 001 \rangle$ zone axis (defocus $\approx -650 \text{ \AA}$). Regions I, II, and III correspond to different thicknesses. (b) Images calculated at the experimental defocus for different thicknesses (20 \AA (a), 40 \AA (b), 60 \AA (c), 80 \AA (d)).

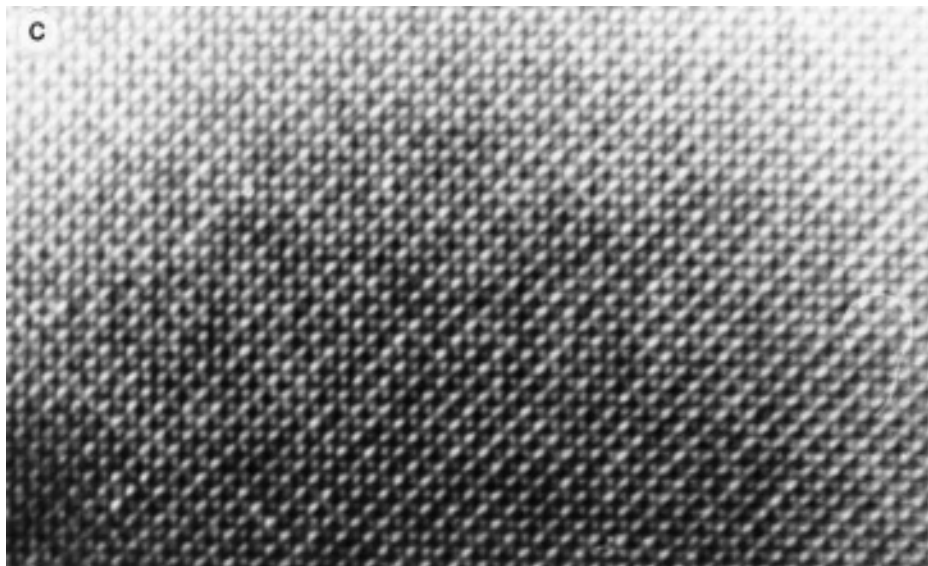
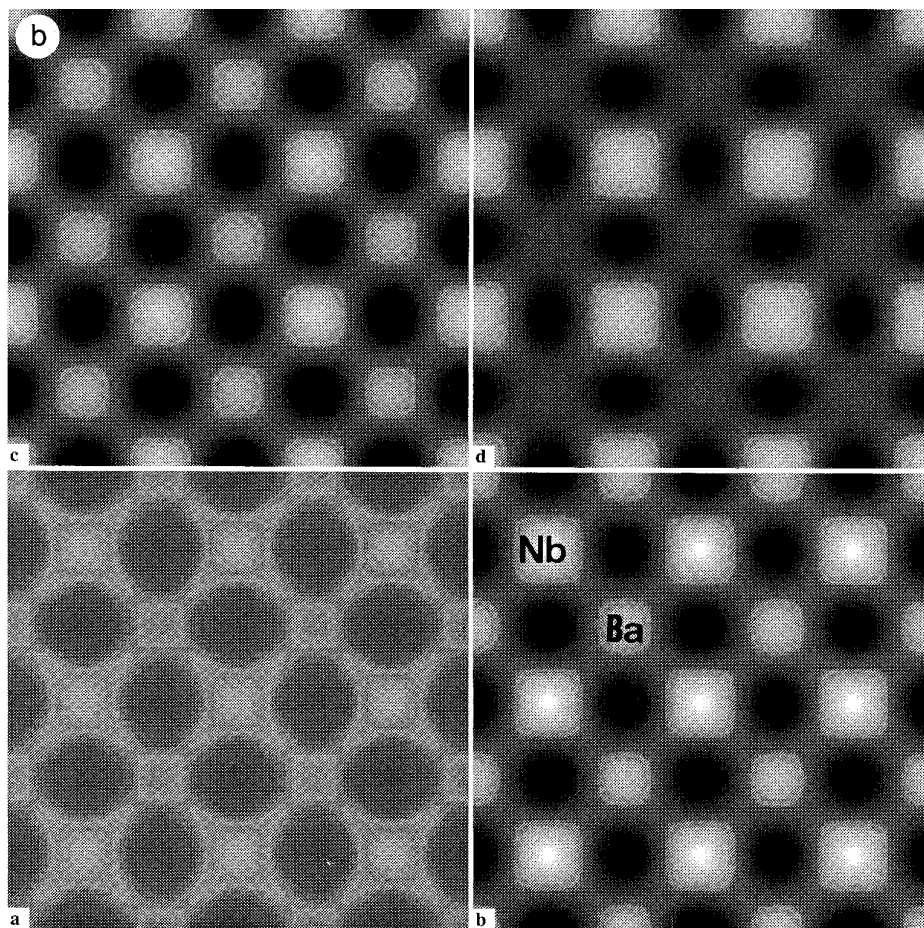


FIG. 4—Continued

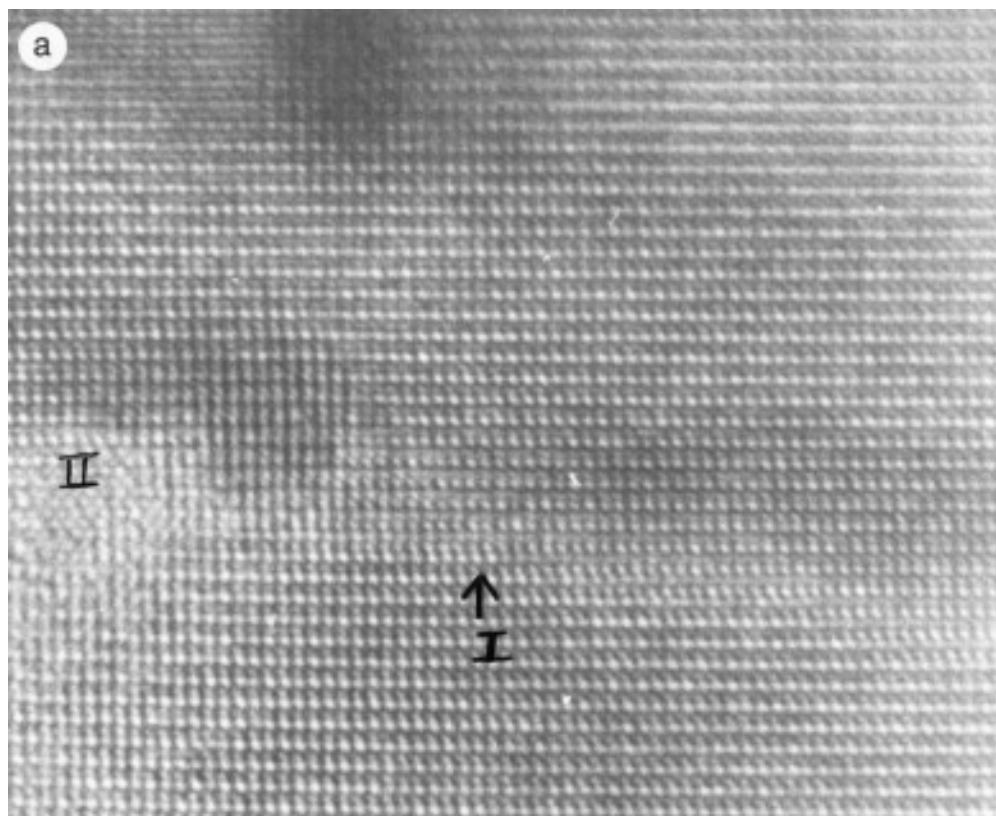


FIG. 5. HREM image of $\text{Ba}_{0.5}\text{K}_{0.5}\text{NbO}_3$ (sample 3) taken along the $\langle 011 \rangle$ zone axis. Zone I corresponds to regions where a $1/2(a + b + c)$ shift occurs. Zone II is at the intersection of two zones I.

the broader the reflections are. This explains the increase of the reflection width observed after the pressure treatment.

b. $\text{K}_{0.5}\text{Ba}_{0.5}\text{NbO}_3$. Figure 4a shows a HREM taken along the $\langle 001 \rangle$ zone axis on a crystallite of $\text{K}_{0.5}\text{Ba}_{0.5}\text{NbO}_3$, with regions of different thicknesses. In region I (near the edge of the sample) large bright dots (A) forming squares centered around smaller white dots (B) can be observed. In region II, both types (A and B) of bright dots have almost the same intensities. In region III, only dots B are present, with a higher intensity than in region I. From image calculations at the experimental defocus value (≈ -650 Å) this variation of contrast can be interpreted as a change in the thickness of the sample from about 40 Å in region I to about 60 Å in region II, and 80 Å in region III. The image calculation is presented in Fig. 4b. In the structural model used, Ba and K atoms have been distributed randomly on the same crystallographic site. In the thinner part (I) of the crystal, the Nb cations correspond to the brightest dots, whereas in the thicker part (III) only the (Ba, K) atoms are imaged. Besides the change in the contrast due to the variation of thickness, the bright dots

are perfectly aligned. The absence of small domains would explain why no splitting was detected in the corresponding diffraction patterns.

c. Defects. A few defects have been detected in some crystallites, as illustrated in the image taken along the $\langle 110 \rangle$ zone axis of a crystallite of BaNbO_3 and shown in Fig. 5a. From the image calculations the present experimental image would correspond to a crystal thickness of ≈ 50 Å and a defocus value of ≈ -800 Å. Ba atoms are imaged as intense white dots. In zone I indicated by the arrow, a shift of $1/(a + b + c)$ occurs. From image calculations this cannot be interpreted as a thickness change as in Fig. 4a, but corresponds to an exchange between the positions of Ba and Nb cations in the structure. Zone II is at the intersection of two regions of type I but with a different orientation, and is therefore a very perturbed area.

CONCLUSION

Electron microscopy studies have shown the presence of small misoriented domains in BaNbO_3 samples. These domains are smaller for the higher pressure treated sam-

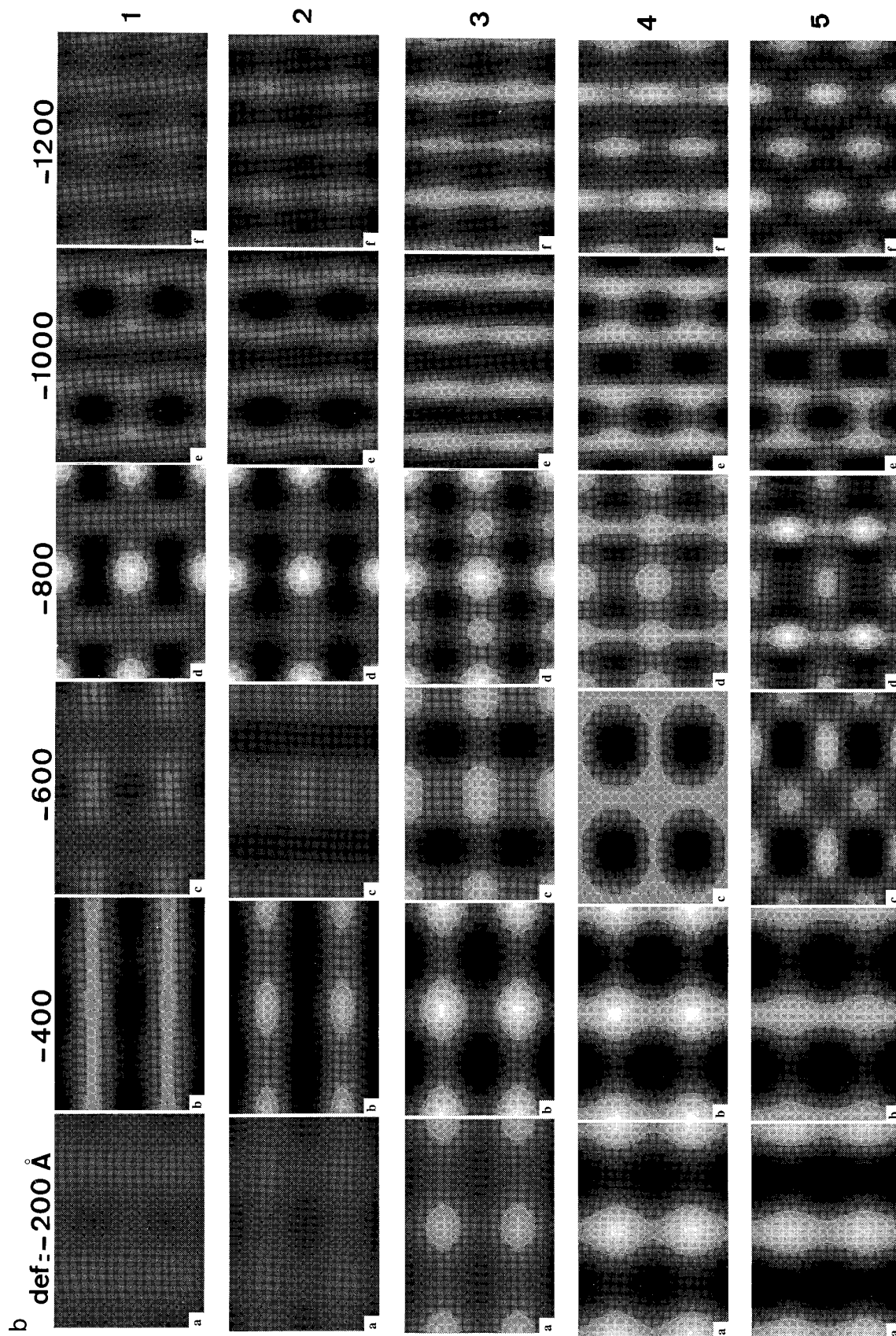


FIG. 5—Continued

ples than for the as-synthesized ones. This observation explains the broadness of the hkl reflections observed by powder X-ray diffraction. From EDS analysis, the (Ba + K)/Nb ratio is equal to 1 for all samples and the cation stoichiometry does not change from one domain to the other. However, one cannot neglect the possible Ba-deficiency at the domain boundaries which could not be detected from EDS analysis. This would explain the small decrease of the lattice constant after the pressure treatment (1). No distortion from the cubic symmetry was detected. In the case of K-doped samples small domains were not observed. The K stoichiometry from different crystallites was found to be quite constant. Neither superstructure reflections nor contrast in the images were observed that could be related to an ordering of K and Ba cations.

REFERENCES

1. E. M. Kopnin, S. Ya. Istomin, O. G. D'yachenko, E. V. Antipov, P. Bordet, J. J. Capponi, C. Chaillout, M. Marezio, S. de Brion, and B. Souletie, *Mater. Res. Bull.* **30**(11), 1379 (1995).
2. E. I. Krylov and A. A. Sharnin, *J. Gen. Chem. U.S.S.R.* **25**, 1637 (1955).
3. D. Ridgley and R. Ward, *J. Am. Chem. Soc.* **77**, 6132 (1955).
4. R. Kreiser and R. Ward, *J. Solid State Chem.* **1**, 368 (1970).
5. B. Hessen, S. A. Sunshine, T. Siegrist, and R. Jimenez, *Mater. Res. Bull.* **26**, 85 (1991).
6. K. Isawa, J. Sugiyama, K. Matsuura, A. Nozaki, and H. Yamauchi, *Phys. Rev. B* **47**, 2849 (1993).
7. M. T. Casais, J. A. Alonso, I. Rasines, and M. A. Hidalgo, *Mater. Res. Bull.* **30**, 201 (1995).
8. P. Stadelmann, *Ultramicroscopy* **21**, 131 (1987).
9. J. A. Alonso, M. T. Casais, and M. J. Mertz-Lopez, *Mater. Res. Bull.* **30**, 251 (1995).